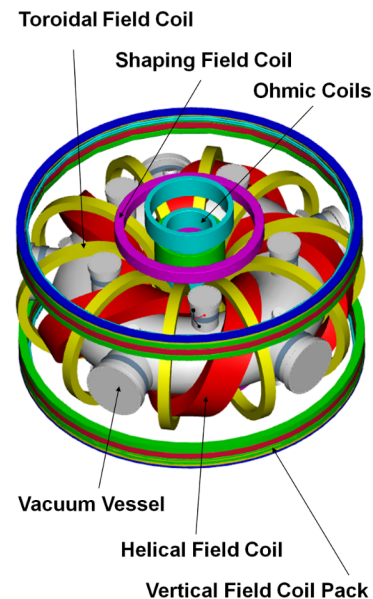
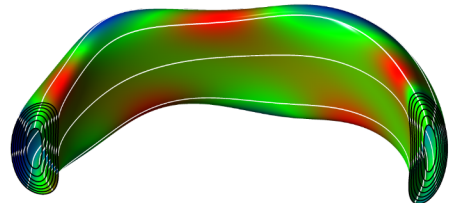


Compact Toroidal Hybrid

The Compact Toroidal Hybrid (CTH) is a torsatron-tokamak hybrid with a helical field coil and vertical field coils to establish a stellarator equilibrium, while an ohmic coil induces plasma current.



A feature of the CTH device is the ability to adjust the vacuum rotational transform, τ_{vac} ($\tau = \frac{1}{q}$), by varying the ratio of current in the helical and toroidal field coils.

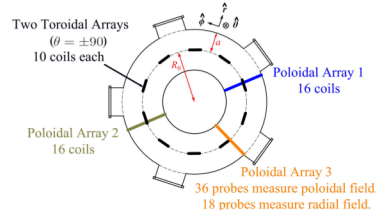


Vacuum flux surfaces generated by external stellarator coils with $\tau_{vac} = 0.05$. White lines are magnetic field lines, and red color represents high magnetic field strength while blue is low. The helical modulation of magnetic field strength is about 0.15 T with $\langle |B| \rangle = 0.5$ T.

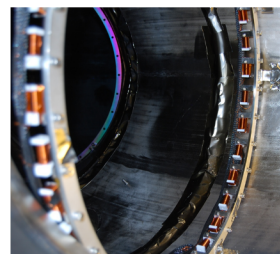
CTH Parameters

$R_0 = 0.75$ m	$a_v = 0.29$ m	$a_{plasma} = 0.2$ m
$B_0 \leq 0.7$ T	$P_{ECRH} \leq 30$ kW	$P_{OH} \sim 200$ kW
$I_p \leq 80$ kA	$n_e \leq 5 \times 10^{19}$ m ⁻³	$T_e \leq 200$ eV
$\tau_{vac}(a) \sim 0.02 - 0.3$	$\beta \leq 0.5\%$	Discharge duration ≤ 0.1 s

Magnetic fluctuations detected with multiple arrays of B_θ pickup coils

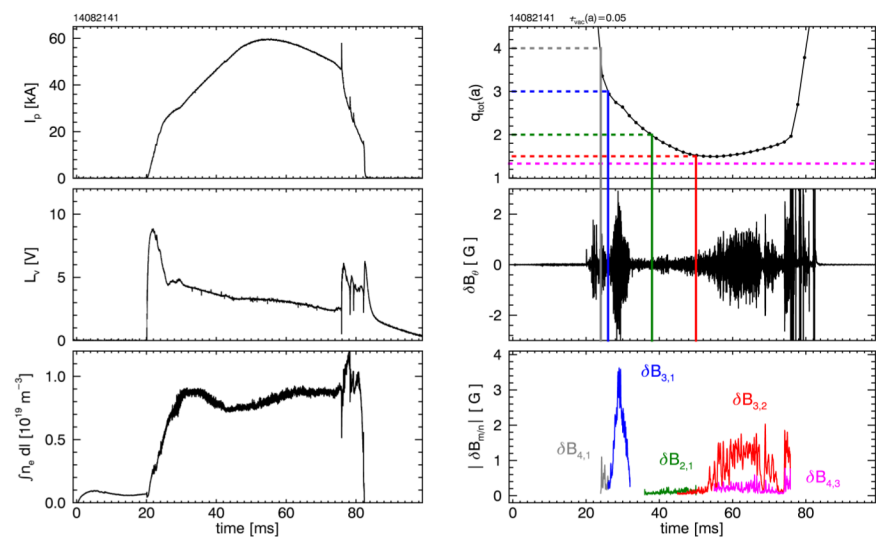


Poloidal and toroidal arrays of pickup coils are used to determine the poloidal (m) and toroidal mode numbers (n).



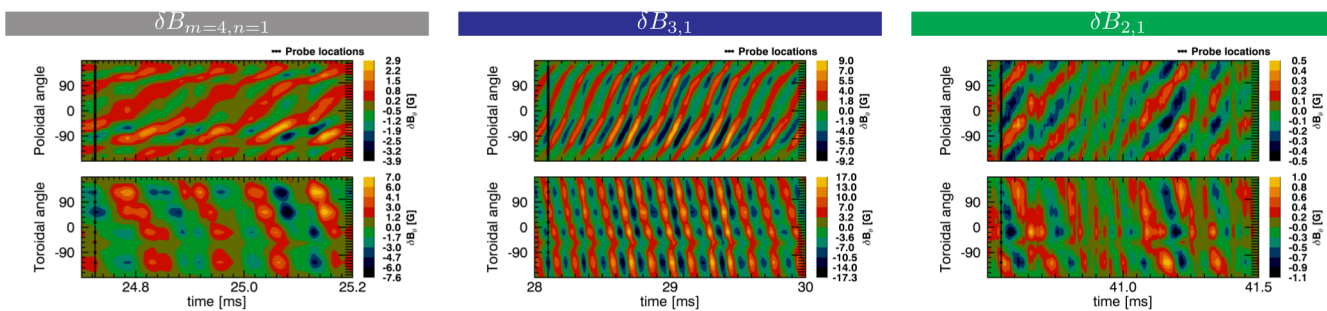
Picture of one of the poloidal arrays installed inside the CTH vacuum chamber is shown here. It has 36 probes that measure the fluctuations in poloidal field.

Low- $q(a)$ disruptions with $q(a) < 2$ characterized by $m=3/n=2$ precursor



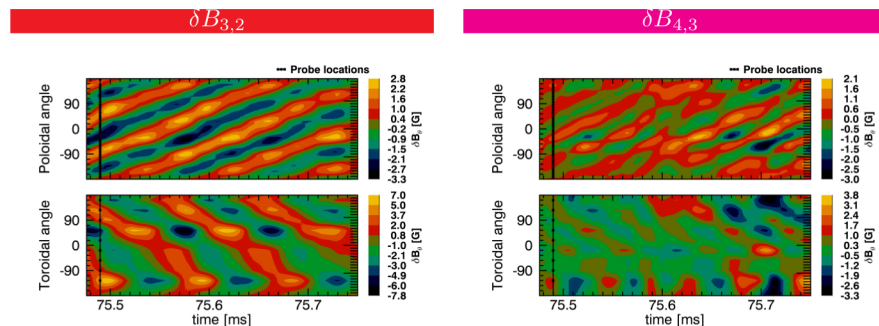
MHD activity during current rise

- Strong current ramp in the initial current rise phase of the discharge with $dI_p/dt \sim 3$ MA/s from $t = 20$ ms to $t = 30$ ms
- Burst of 4/1 and 3/1 activity observed during this initial phase
- $dI_p/dt \sim 1$ MA/s from $t = 30$ ms to $t = 50$ ms
- Strong current gradients present as 2/1 surface moves out into the vacuum

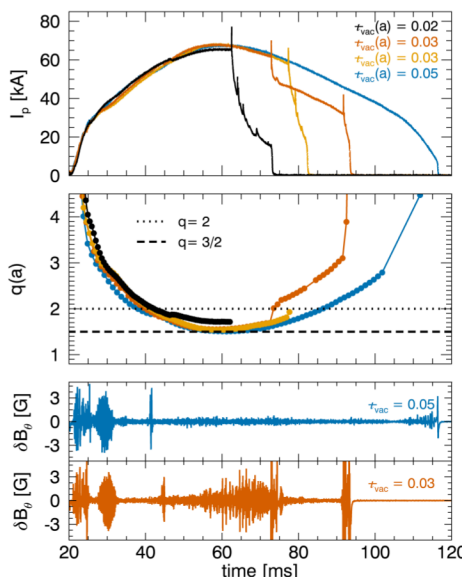


3/2 and 4/3 modes grow prior to disruption

- Biorthogonal decomposition [5] is used to separate 3/2 and 4/3 modes from total fluctuations in δB_θ .
- Frequency of 3/2 mode is $\sim 10 - 12$ kHz.
- Frequency of 4/3 mode is $\sim 18 - 19$ kHz.



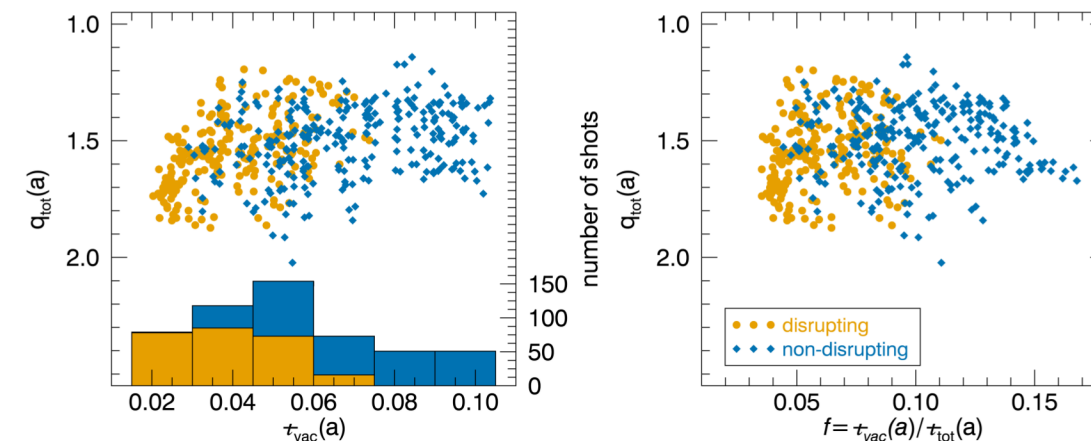
Disruptivity changes with addition of τ_{vac}



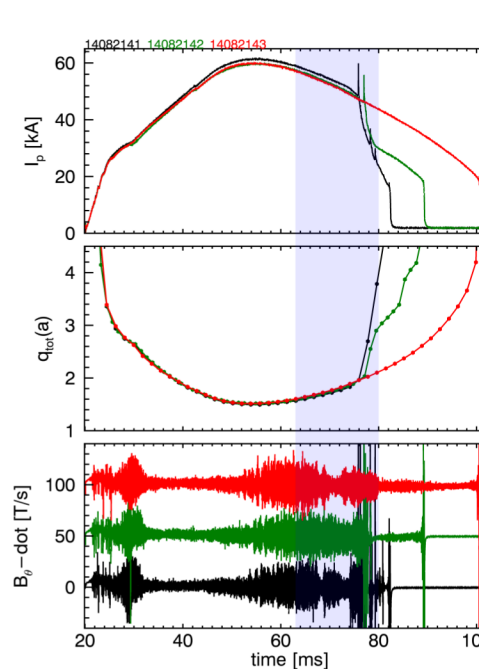
- τ_{vacuum} can be changed by changing the currents in the external coils of CTH, specifically the ratio of currents in helical field coil (HF) and the toroidal field coil (TF).
- The figure shows discharges with different values of vacuum transform, but with similar evolution of the total plasma current.
- Total rotational transform, $t_{tot} = \tau_{vacuum} + \tau_{current} = \frac{1}{q}$, is maintained approximately constant.
- Magnetic fluctuation activity between cases of $\tau_{vac} = 0.03, \tau_{vac} = 0.05$ is shown.
- About 95% of the contribution to t_{tot} , is from the plasma current.
- Fractional transform is defined as $f = \tau_{vacuum} / t_{tot}$, with t_{tot} computed at peak plasma current.
- τ is computed from 3D equilibrium reconstruction code V3FIT [2] using data from only the magnetic diagnostics.

Disruptions suppressed for $f \gtrsim 0.1$

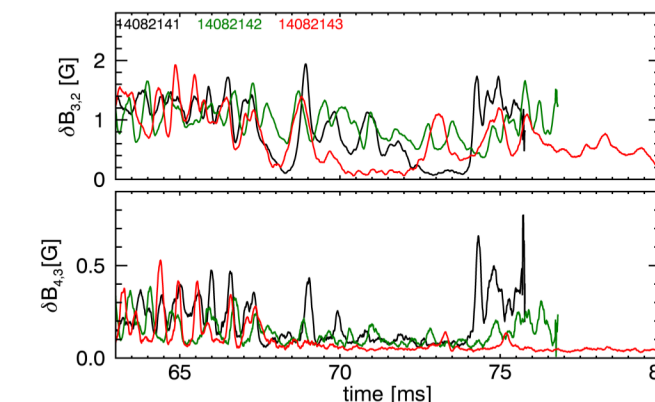
- About 500 shots are taken for a range of values of $\tau_{vac}(a)$ and t_{tot} .
- Disruptions are suppressed as $\tau_{vac}(a)$ is raised to 0.07.



$m=3/n=2$ and $m=4/n=3$ modes are dominant disruption precursors



Comparison of shots at fixed value of $\tau_{vac}(a) = 0.05, f \sim 0.3$



- Three shots have similar evolution of $q(a)$ and I_p .
- Growing 3/2 and 4/3 modes lead to a disruption in two shots. For third shot, 3/2 and 4/3 remain small and disruption is not observed.

Comments

- CTH operates beyond the traditional tokamak limit of $q(a) > 2$. Low- $q(a)$ disruptions on CTH are driven by 3/2 and 4/3 modes.
- The conjecture to explain the suppression there was that the addition of vacuum transform shifts the location of the rational surface to a region of less steep current gradient and hence increased stability.
- A threshold for disruption suppression is observed at a modest fractional transform of about 0.1
- Hybrid machines in past have observed disruption suppression of the 2/1 mode at levels of $\tau_{vac} \sim 0.14$ [6].
- We think that a similar mechanism might be responsible for disruption suppression in CTH. Knowledge of current profile for CTH will give a clear picture of the mechanism.

References

- M. D. Pandya, M. C. ArchMiller, M. R. Cianciosa, D. A. Ennis, J. D. Hanson, G. J. Hartwell, J. D. Hebert, J. L. Herfindal, S. F. Knowlton, X. Ma, S. Massidda, D. A. Maurer, N. A. Roberds and P. J. Traverso, Phys. Plasmas **22**, 110702 (2015)
- J. D. Hanson, S. P. Hirshman, S. F. Knowlton, L. L. Lao, E. A. Lazarus, and J. M. Shields, Nucl. Fusion **49**, 075031 (2009).
- Hirshman S.P., Lazarus A., Hanson J.D., Knowlton S.F. and Lao L.L., Phys. Plasmas **11**, 595 (2004).
- G. Y. Fu, L. P. Ku, W. A. Cooper, S. H. Hirshman, D. A. Monticello, M. H. Redi, A. Reiman, R. Sanchez and D. A. Spong, Phys. Plasmas **7**, 1809 (2000).
- T. Dudok de Wit, A. Pecquet, J. Vallet, and R. Lima, Phys. Plasmas **1**, 3288 (1994).
- W VII-A Team, Nucl. Fusion **20**, 1093 (1980)

Acknowledgement: This work is supported by the USDoE under grant DE-FG02-00ER54610.

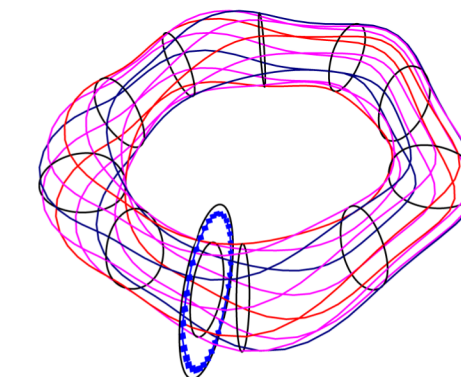
Modeling MHD fluctuations in CTH

- Interpretation of spatial structure of MHD fluctuations in CTH difficult because of
 - the toroidal nature of the plasma
 - non-axisymmetry of the stellarator fields
- Biorthogonal decomposition [5] is an empirical tool to interpret mode structures but does not incorporate any information from the equilibrium.

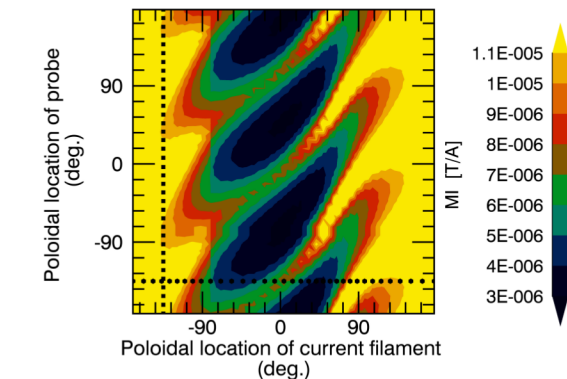
Observed MHD modes modeled as current filaments on rational surface

$$\begin{aligned} \text{Model signal: } S_i^M &= \sum_{j=0}^{N_f} M_{i,j} I_j \\ \text{Filament current model: } I_j &= I_0 \sin(m\theta_j + \delta) \\ \text{Fitting observed sig. } S_i^O: \chi^2 &= \sum_{i=0}^{N_D} \left[\frac{S_i^M - S_i^O}{\sigma_i} \right]^2 \end{aligned}$$

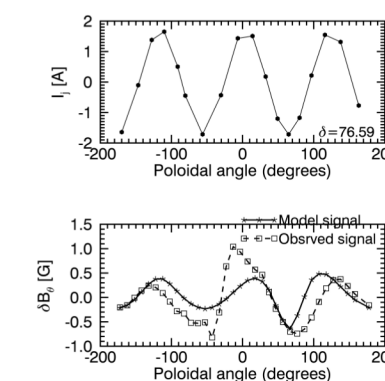
4 filaments on rational surface with $\tau = 2/3$. Each filament goes around three times toroidally and twice poloidally. The rational surface at half and full periods in CTH are shown. The location of b-dot probes is shown in blue.



M_{ij} , mutual inductances between pickup coils and filaments computed with V3RFUN code [3]



Model with filament-currents I_j to match observed signals S_i^O



Future work would include better filament model and incorporating other existing poloidal and toroidal arrays of pickup coils.